

Improved Monte-Carlo Simulator of Partial Discharge

R. J. Van Brunt and P. von Glahn

National Institute of Standards and Technology
Gaithersburg, MD 20899 USA

Abstract

A previously introduced Monte-Carlo simulator of partial discharge (PD) has been extended and made more versatile to allow simulation of a wider range of observed discharge behavior. The version of the simulator described here allows simulation of pulsating PD that can be represented as a point process and covers such properties as nonstationary behavior associated with PD-induced modifications of the discharge site and statistical characteristics of multi-site discharges. In the present work, it is shown how the simulator can be applied to gain insight into the physical basis for the previously reported anomalous stochastic behavior of PD generated by applying low-frequency alternating voltages to point electrodes that touch the surface of pure Al_2O_3 .

Introduction

Monte-Carlo simulators of pulsating partial-discharge PD have been used in recent years to gain physical insight into the observed statistical characteristics of this phenomenon [1-5] that cannot be gained from deterministic models [6]. The present work discusses an extension of a Monte-Carlo PD model originally proposed by Van Brunt and Cernyar [3] that allows greater flexibility for including effects such as those resulting from different discharge initiation mechanisms, multiple discharge sites, discharge-produced aging, dynamics of charging on dielectric surfaces, and variations in the statistics of discharge growth. The PD simulator described here can be used to interpret statistical results from PD measurements, to validate algorithms for performing stochastic analysis of recorded PD data, and to test proposed PD pattern recognition schemes such as those based on neural networks. The simulator also generates binary data files identical in format to those produced by a PD digitizer-recorder system [7].

A description of the simulator is provided together with an example of its application to the interpretation of recent experimental results reported about the unusual behavior of PD generated by applying an alternating voltage to a sharp electrode that touches surfaces of high-purity aluminum oxide (Al_2O_3) [8].

Description of the Simulator

The simulation is based on the assumption that the discharge can be treated as a random point process which, for an alternating applied voltage, is represented by a set of numbers $\{\phi_{i,j}^{\pm}, q_{i,j}^{\pm}, j\}$ where $\phi_{i,j}^{\pm}$ is the phase of occurrence of the i th positive or negative PD pulse in the j th voltage cycle and $q_{i,j}^{\pm}$ is the corresponding amplitude of that pulse (see Fig. 1). The assumption of a point process implies that the width of the PD pulses are infinitesimally small compared to the period, T of the applied voltage. The time

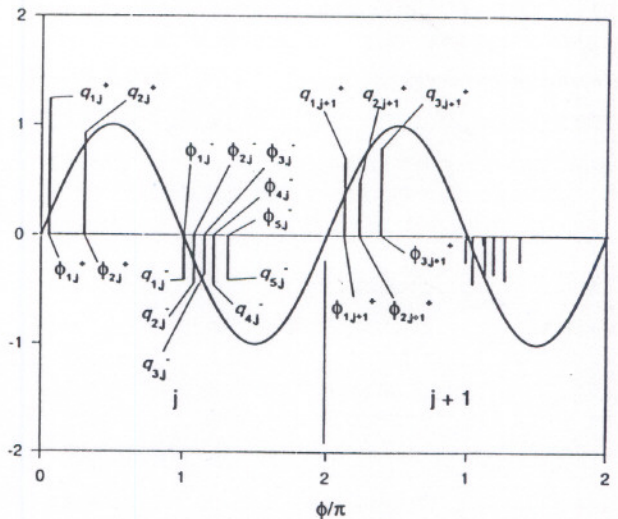


Figure 1 - Definitions of phases, $\phi_{i,j}^{\pm}$, and amplitudes, $q_{i,j}^{\pm}$ of PD pulses associated with two successive cycles (j and $j + 1$) of the applied voltage.

of occurrence of a PD event as measured from the beginning of the simulation is given by

$$t_{i,j}^{\pm} = (j - 1 + \phi_{i,j}^{\pm}/2\pi)T. \quad (1)$$

When a PD pulse occurs, it is assumed to reduce the local electric-field strength at the discharge site by an amount $|\Delta E_{i,j}^{\pm}(t_{i,j}^{\pm})|$ which is directly proportional to $|q_{i,j}^{\pm}|$.

The local, time-dependent field at the k th discharge site is written as

$$E_k(t) = E_{a,k}(t) - \Delta E_k(t), \quad (2)$$

where the first term on the right-hand side is the externally applied field and the second term corresponds to the net, accumulated local field reduction up to time t given by

$$\Delta E_k(t) = \sum_{j=1}^{J_t} \left[\sum_{i=1}^{n_j^+} \Delta E_{i,j,k}^+(t_{i,j}^+) - \sum_{i=1}^{n_j^-} \Delta E_{i,j,k}^-(t_{i,j}^-) \right], \quad (3)$$

where n_j^+ is the number of positive PD events in the j th cycle and n_j^- is the number of negative PD events in that same cycle. It is implied in Eq. (3) that the cycle $j = J_t$ occurs at time t , so that $t \geq t_{i,j}^{\pm}$ for all events included in the summation over j . Although any periodic form can be used for the applied field, it is assumed in the example below to be sinusoidal with a possible bias, $\alpha E_{0,k}$, due to a permanent or quasi-permanent surface charge of a preferred sign, i.e.,

$$E_{a,k}(t) = E_{0,k} \sin \omega t + \alpha E_{0,k} \quad (4)$$

where $\omega = 2\pi/T$ and typically $|\alpha| < 1$.

In cases where more than one PD site are included, each site can have different characteristics that control discharge initiation and growth. The individual sites are assumed to be non-interacting, i.e., the behavior of PD at one site is not correlated with the occurrence of PD at other sites. The PD pulses from the individual sites are superimposed in the output of the simulation.

Each cycle is divided into a large number of equal time intervals, Δt , where $T/\Delta t$ is typically greater than 1000. When the time is increased from t to $t + \Delta t$, a subroutine is called to determine if a PD event can occur. It is assumed that an event can occur if an initiatory electron is released at the discharge site. The rate of electron release at the site, $r_{e,k}^{\pm}(|E_k(t)|)$, is assumed to increase with increasing

local electric-field strength, and can, in general, depend on the polarity of the applied field. Different models, such as the field-emission model used previously [3,4], can be assumed for the field dependence of the electron emission rate. "Aging" effects can be simulated by allowing the electron emission rates to change with cumulative discharge exposure, as measured, for example, by the net PD positive or negative charge up to a time t .

The probability, $p'_{\pm}(t)dt$, that an electron will be released in the time interval t to $t + dt$ is proportional to $r_{e,k}^{\pm}$ and given by

$$p'_{\pm}(t)dt = r_{e,k}^{\pm}(|E(t)|) \left[1 - \int_0^t p'_{\pm}(t')dt' \right] dt. \quad (5)$$

If t lies within the increment Δt during which $r_{e,k}^{\pm}$ can be taken as a constant, one obtains

$$p_{\pm}(\Delta t) = \int_0^{\Delta t} p'_{\pm}(t')dt' = 1 - \exp(-r_{e,k}^{\pm} \Delta t) \quad (6)$$

or

$$p_{\pm}(\Delta t) \simeq r_{e,k}^{\pm} \Delta t \quad (7)$$

for the probability that a positive or negative-PD pulse will be initiated during the time Δt .

After each incremental increase of time, the value of $p_{\pm}(\Delta t)$, computed using an assumed model for electron release, is compared with a random number, R , between 0 and 1. If $R \leq p_{\pm}(\Delta t)$, then an initiatory electron is assumed to be released during Δt .

Once it is determined that a PD event can occur, the amplitude, $q_{i,j}^{\pm}$, of the event is computed according to a statistical model for discharge growth in which the mean value of $|q_{i,j}^{\pm}|$ at any discharge site is assumed to increase with increasing local field strength. Previous models [3] invoked a normal distribution for discharge growth statistics.

In the simulation considered here of PD generated on Al_2O_3 surfaces, the amplitude of a PD pulse was calculated according to the prescription:

$$|q_{i,j}^-| = \mu + \beta_0 \sigma x + \beta_1 |x| \quad (8)$$

where

$$x = (2R_1 - 1)[-2 \log(S)/S]^{1/2}, \quad (9)$$

$$S = (2R_1 - 1)^2 + (2R_2 - 1)^2, 1 > S > 0 \quad (10)$$

$$\mu = \beta_2 E_0 + \beta_3 R_3 (\alpha E_0 - \Delta E_k) \quad (11)$$

and

$$\sigma = \beta_4 (\alpha E_0 - \Delta E_k). \quad (12)$$

The factors β_k , $k = 0$ to 4 are adjustable positive constants, and R_ℓ , $\ell = 1$ to 3 are independent random numbers between 0 and 1. The form given by Eqs. (8)–(12) yields asymmetric, quasi-normal amplitude distributions. The amplitude distributions become Gaussian in the limit where $\beta_1 = \beta_3 = 0$.

Stochastic Analysis

The results from the simulation can be subjected to the same kind of stochastic analysis as experimental results obtained from continuous recordings of PD [7,8]. In the example considered below, the amplitude and phase distributions of negative-PD pulses selected according to their order of occurrence in a cycle, were determined from the set of random variables $\{\phi_{i,j}^-, q_{i,j}^-, j\}$ generated by the simulator. The distributions were determined by sorting the data into evenly spaced sets of adjoining, but non-overlapping intervals Δq_ℓ^- and $\Delta \phi_\ell^-$, where each set consists of M_ℓ intervals. The distributions in phase and amplitude of the i th negative-PD pulse are given respectively by

$$P(\phi_i^-, \Delta \phi_\ell^-) = \sum_{j=1}^N \frac{m_j(\phi_{i,j}^-, \Delta \phi_\ell^-)}{N} \quad (13)$$

and

$$P(q_i^-, \Delta q_\ell^-) = \sum_{j=1}^N \frac{m_j(q_{i,j}^-, \Delta q_\ell^-)}{N} \quad (14)$$

where N is the number of cycles included in the simulation. It is required that $m_j(\phi_{i,j}^-, \Delta \phi_\ell^-) = 1$ if $\phi_{i,j}^- \in \Delta \phi_\ell^-$, otherwise $m_j(\phi_{i,j}^-, \Delta \phi_\ell^-) = 0$. In the cases where at least i pulses occur in the j th cycle, the sum over all intervals satisfies the condition

$$\sum_{\ell=1}^{M_\ell} m_j(\phi_{i,j}^-, \Delta \phi_\ell^-) = 1, \quad (15)$$

which means that $\phi_{i,j}^-$ can be contained in one and only one phase interval of the set $\Delta \phi_\ell^-$. A similar requirement applies to $m_j(q_{i,j}^-, \Delta q_\ell^-)$. The probability, $P(\phi_i^-, \Delta \phi_\ell^-)$, that any negative-PD pulse lies in the window $\Delta \phi_\ell^-$ regardless of its order of occurrence is given by the sum

$$P(\phi_i^-, \Delta \phi_\ell^-) = \sum_{i=1}^{n_k^-(\max)} P(\phi_i^-, \Delta \phi_\ell^-), \quad (16)$$

where $n_k^-(\max)$ is the largest number of negative-PD pulses that was ever recorded for any cycle. A similar expression is used to obtain the unconditional amplitude distributions, $P(q_i^-, \Delta q_\ell^-)$, for all negative-PD pulses.

Example of a Simulation - PD on Al₂O₃ Surfaces

In this section we consider an example of results from the simulator applied to the interpretation of the anomalous behavior of PD that have been observed [8] in the case where an alternating sinusoidal voltage is applied to a sharply pointed electrode that touches the surface of high-purity (99.9%) Al₂O₃. It was found for this material that the positive-PD pulses cease within less than a minute after the voltage is applied, after which time, negative-PD pulses continue to occur in a relatively stationary pattern for an indefinite time and the mean number of PD pulses per cycle increases with the applied voltage.

Examples of the phase and amplitude distributions, $P(\phi_i^-, \Delta \phi_\ell^-)$, and $P(q_i^-, \Delta q_\ell^-)$, for 99.9% Al₂O₃ at 2.5 kV rms and 70 Hz are shown respectively in Figs. 2 and 3. These data correspond to the selected 120 s time windows indicated on the figures after cessation of the positive-PD pulses has occurred. The data in these figures have been arbitrarily normalized to the maximum numbers of events that occurred in any interval $\Delta \phi_\ell^-$ or Δq_ℓ^- . It is seen that the discharge was relatively stationary for least 40 min after application of the voltage, i.e., no significant changes occurred in the recorded distributions for the individually selected PD pulses. The widths of the phase and amplitude distributions as well as the mean values of the phase and amplitudes of the individual negative-PD pulses increase with increasing pulse number, i . The phase of the first negative pulse has a mean centered about the applied-voltage zero crossing, i.e., $\langle \phi_1^- \rangle \simeq \pi$.

Shown in Fig. 4 are examples of experimental results [8] for the negative-PD phase distributions obtained at two different voltages which indicate that the number of events per cycle increases with the voltage. Also shown in this figure are the distributions, $P(\phi_i^-, \Delta \phi_\ell^-)$ for all events as given by Eq. (16).

Figures 5 and 6 show examples of phase and amplitude distributions respectively of individual negative-PD pulses obtained from the simulator under conditions designed to approximate the experimental re-

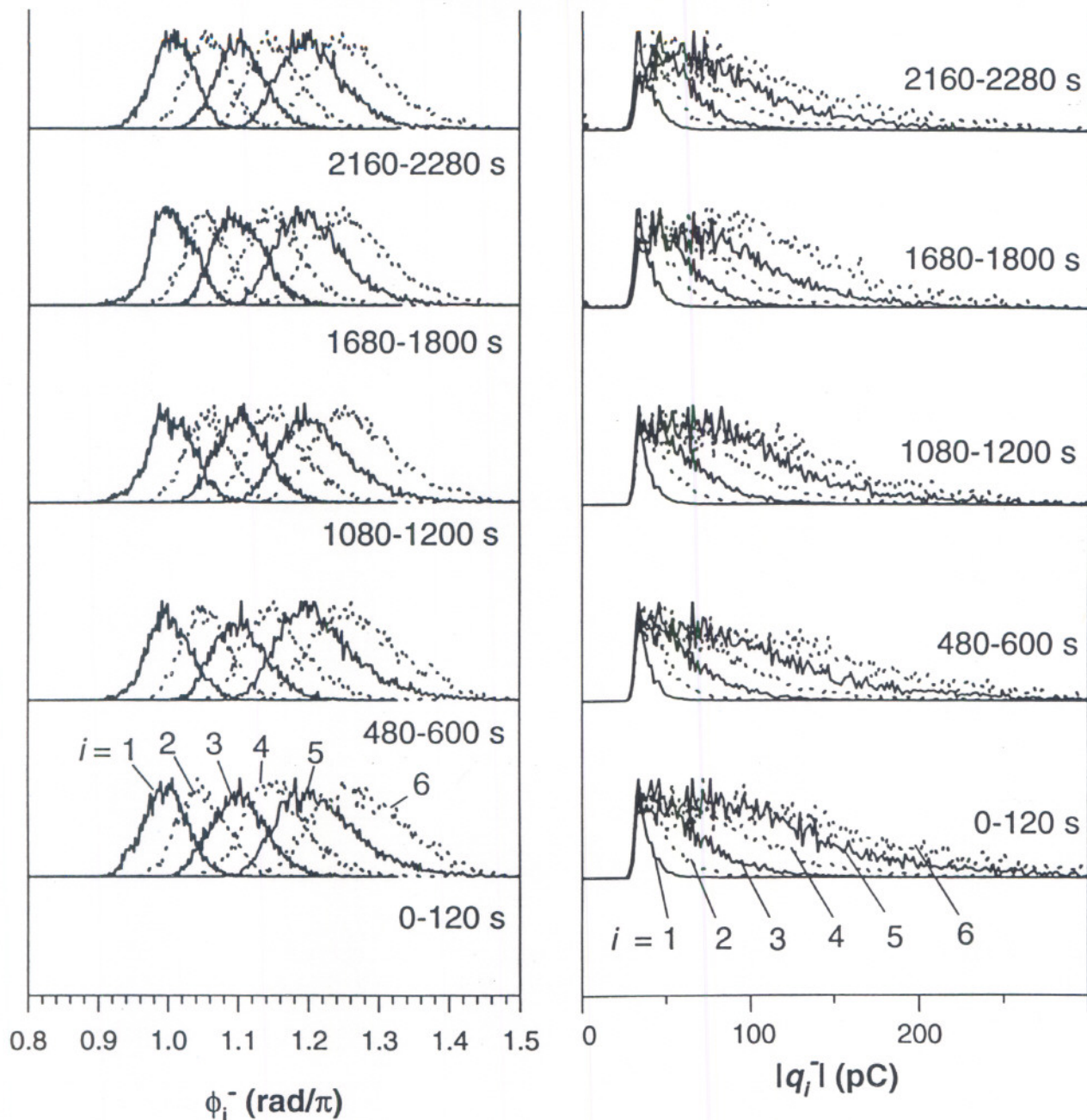


Figure 2 - Measured phase distributions of the individually selected negative-PD pulses generated by applying 2.5 kV rms, 70 Hz voltage to a point electrode touching a 99.9% Al₂O₃ surface for the indicated 120 s time intervals after cessation of the positive-PD pulses [8]. The distributions have been normalized to their maximum values.

Figure 3 - Measured amplitude distributions for the negative-PD pulses that correspond to the phase distributions shown in Fig. 2. The distributions have been normalized to their maximum values [8].

sults shown in Figs. 2-4 at 2.5 kV. As for the simulation of PD on epoxy surfaces [4,5], it was found that the positive PD will cease if: 1) the negative surface charge, proportional to $\Delta E(t)$ ($\Delta E(t) < 0$), is allowed to decay according to the prescription

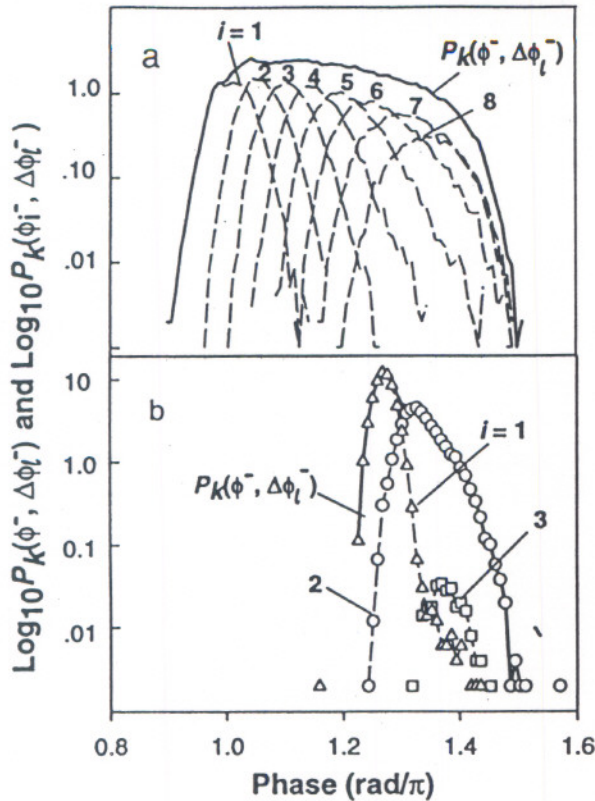


Figure 4 - Examples of measured phase distributions of negative-PD pulses for 99.9% Al_2O_3 : a) 70 Hz, 2500 V rms; b) 150 Hz, 800 V rms [8].

$$\Delta E(t + \Delta t) = \Delta E(t) \exp(-\Gamma |E(t)| \Delta t / E_0) \quad (17)$$

where Γ is a decay constant that satisfies the condition $\Gamma > 2\pi\omega$; and 2) the probability of initiatory electron release from the surface increases with increasing negative surface-charge density.

Two additional assumptions were required to explain the Al_2O_3 results shown here. First, in order to account for the fact that, at higher voltages, the mean phase of the first negative-PD pulse is centered at the zero crossing, it was necessary to allow the surface charge to build up during the positive half cycle to a value that nearly cancels the applied field, i.e., it was necessary to take $\alpha \simeq 1$ in Eq. (4). Secondly, to account for the increases in the mean values and widths of the amplitude distributions with i , as seen in Fig. 2, it was necessary to allow the parameters μ and σ to increase with increasing $|\Delta E|$. This is implied in the forms of Eqs. (11) and (12), and essentially means that the charge deposited on the

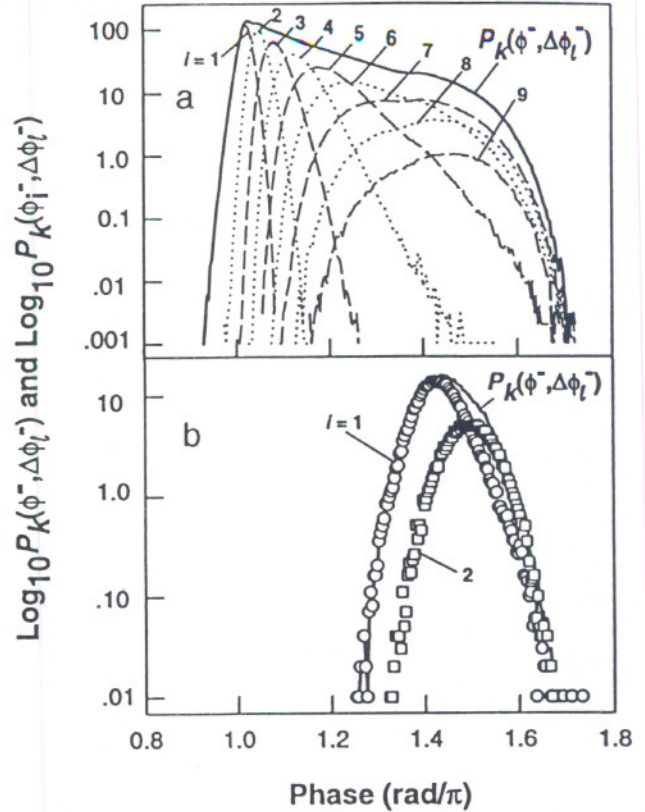


Figure 5 - Phase distributions for individual and all negative-PD pulses obtained using simulator model parameters that yield a behavior similar to the experimental results given in Figs. 2 and 4. The results in (a) were obtained at a higher applied field than the results in (b).

dielectric surface by a particular negative-PD event randomizes the local electric field at the discharge site where subsequent PD pulses develop. Significant increases of $\langle q_i^- \rangle$ with i also imply that the local field reduction, $\Delta E_{i,j}^-$, due to a negative-PD pulse can only be a relatively small fraction of E_0 as determined by the parameters β_2 and β_3 in Eq. (11). In all cases, the amplitude of any PD is constrained to have an upper limit imposed by the necessity to avoid non-physical electric-field reversal at the discharge site.

It should be noted that if $\alpha = 0$, then the results of a simulation that yields the same mean number of negative-PD pulses per cycle as in Fig. 5a give a value for $\langle \phi_1^- \rangle$ that is significantly greater than π . When E_0 is reduced to a value close to PD inception, then, as seen in Fig. 5b, the mean number of nega-

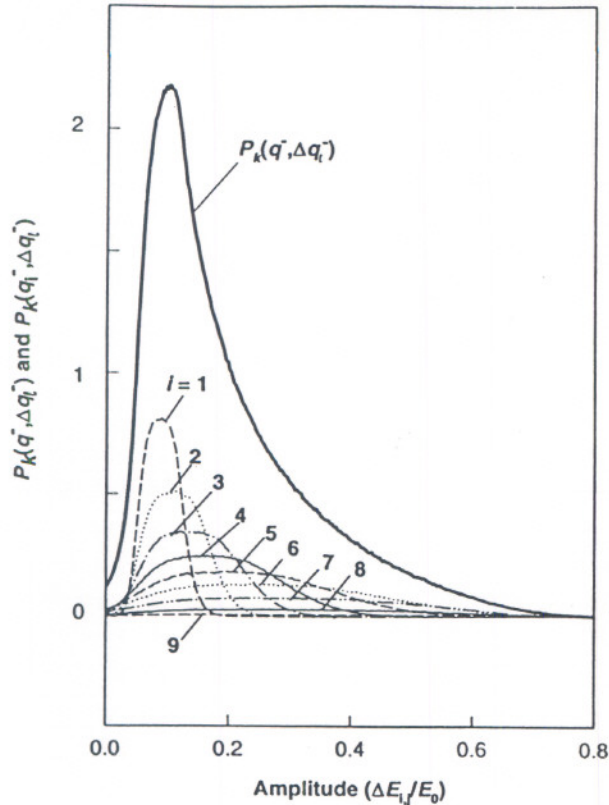


Figure 6 - Amplitude distributions of simulated PD corresponding to the phase distributions presented in Fig. 5a.

tive PD per cycle decreases in accordance with the experimental results shown in Fig. 4. For the case presented in this figure, it was found that a lower value of $\alpha = 0.3$ together with a higher value for β_2 produced behavior most like the experimental results. There is, in fact, no physical requirement that the parameters such as α and β_2 be independent of the applied field.

Finally, it should be pointed out that the shapes of the amplitude distributions from the simulation presented in Fig. 6 do not precisely match those of the observed distributions in Fig. 3 which show a more abrupt cutoff at the low end. This cutoff is believed to be largely an artificial consequence of the preset discrimination level of PD detector that was used. However, if the cutoff is "real", then a truncated Poisson distribution was found to yield amplitude distribution profiles that look more like the experimental data.

Acknowledgments

This work was performed in the Electricity Division, Electronics and Electrical Engineering Laboratory, National Institute of Standards and Technology, Technology Administration of the U.S. Department of Commerce. Partial support was provided by the U.S. Nuclear Regulatory Commission and by the U.S. Air Force-Wright Patterson AFB.

References

- [1] - B. Fruth and L. Niemeyer, "The Importance of Statistical Characteristics of Partial Discharge Data", IEEE Trans. Elec. Insul., Vol. 27, pp. 60-69, 1992.
- [2] - R. S. Sigmond, "Fast Image Converter and Slow Computer Simulation Studies of Partial Discharge Models", Proc. Int. Conf. on Partial Discharge, IEE Publ. 378 (1993) pp. 15-16.
- [3] - R. J. Van Brunt and E. W. Cernyar, "Stochastic Analysis of ac-generated Partial Discharge Pulses from a Monte-Carlo Simulation", 1992 Annual Report - Conference on Electrical Insulation and Dielectric Phenomena, IEEE, NY, pp. 427-434, 1992.
- [4] - R. J. Van Brunt, "Physics and Chemistry of Partial Discharge and Corona", IEEE Trans. Diel. Elec. Insul., Vol. 1, pp. 761-784, 1994.
- [5] - R. J. Van Brunt, P. von Glahn, and T. Las, "Nonstationary Behaviour of Partial Discharge During Discharge Induced Aging of Dielectrics", IEE Proc.-Sci. Meas. Technol., Vol. 142, pp. 37-45, 1995.
- [6] - R. Schifani, "A Novel Histogram for Partial Discharge Signals in HV Insulating Systems", IEEE Trans. Elec. Insul., Vol. EI-21, pp. 89-99, 1986.
- [7] - P. von Glahn and R. J. Van Brunt, "Continuous Recording and Stochastic Analysis of PD", IEEE Trans. Diel. Elec. Insul., Vol. 2, pp. 590-601, 1995.
- [8] - P. von Glahn, R. J. Van Brunt, and T. Las, "Behavior of Surface Partial Discharge on Aluminum Oxide Dielectrics", 1995 Annual Report - Conference on Electrical Insulation and Dielectric Phenomena, IEEE, NY pp. 365-371, 1995.